INTERNATIONAL JOURNAL OF CLIMATOLOGY
Int. J. Climatol. **27**: 81–91 (2007)
Published online 23 June 2006 in Wiley InterScience
(www.interscience.wiley.com) DOI: 10.1002/joc.1373

Evaluation of snow/ice albedo parameterizations and their impacts on sea ice simulations

Jiping Liu,[a,b,c]* Zhanhai Zhang,[b] Jun Inoue[d] and Radley M. Horton[e]

[a] *State Key Laboratory of Numerical Modeling for Atmospheric Sciences and Geophysical Fluid Dynamics, Institute of Atmospheric Physics, Chinese Academy of Sciences, 100029, China*
[b] *Key Laboratory for Polar Science, Polar Research Institute of China, Shanghai, 200129, China*
[c] *School of Earth & Atmospheric Sciences, Georgia Institute of Technology, Atlanta, GA 30332, USA*
[d] *Institute of Observational Research for Global Change, Japan Agency for Marine-Earth Science and Technology, Yokosuka, 237-0061, Japan*
[e] *Department of Earth and Environmental Sciences, Columbia University, and NASA Goddard Institute for Space Studies, New York, NY, 10025, USA*

Abstract:

Climate models use a variety of snow/ice albedo parameterizations for the ice covered ocean. In this study, we applied *in situ* measurements (surface temperature, snow depth and ice thickness) obtained from the Surface Heat Budget of the Arctic Ocean (SHEBA) as input values to four different snow/ice albedo parameterizations (representing the spectrum of parameterizations used in stand-alone sea ice models, numerical weather prediction and regional climate models of the Arctic Basin, and coupled global climate models), and evaluated the parameterized albedos against the SHEBA observed albedo. Results show that these parameterizations give very different representations of surface albedo. The impacts of systematic biases in the input values on the parameterized albedos were also assessed. To further understand how sea ice processes are influenced by differences in the albedo parameterizations, we examined baseline sea ice characteristics and responses of sea ice to an external perturbation for the simulations of the albedo parameterizations using a stand-alone basin-scale dynamic/thermodynamic sea ice model. Results show that an albedo treatment of sufficient complexity can produce more realistic basin-scale ice distributions, and likely more realistic ice responses as climate warms. Copyright © 2006 Royal Meteorological Society

KEY WORDS snow/ice albedo parameterizations; SHEBA; sea ice model

Received 5 July 2005; Revised 7 May 2006; Accepted 9 May 2006

1. INTRODUCTION

Observations and climate modeling results have indicated that the Arctic is a region of particular importance and vulnerability to global climate change (e.g. Houghton *et al*., 2001). The variation in snow/ice albedo is one of the most important factors influencing the Arctic energy budget and the stability of the Arctic sea ice (e.g. Curry *et al*., 1995; Houghton *et al*., 2001). Increased surface temperature may cause a reduction in the area covered by snow/ice, which would in turn allow increased absorption of solar radiation within the Arctic Ocean and a further increase in surface temperature. This destabilizing process is known as the ice albedo feedback. The projected strong warming in the Arctic associated with increased loading of greenhouse gases in the atmosphere by current-day climate models is at least partly attributed to this feedback mechanism (e.g. Washington and Meehl, 1986; Ingram *et al*., 1989; Houghton *et al*., 2001). Although the ice albedo feedback is counteracted by a stabilizing process (the rate of heat loss at the surface through upward longwave radiation and turbulent heat fluxes increases with increasing surface temperature) to some extent, it becomes increasingly important as the surface temperature in the Arctic approaches the melting point (changing the ice covered ocean to open water) in a gradually warming climate. Therefore, the correct determination of the snow/ice albedo in climate models is one of the essential issues for proper treatment of the ice albedo feedback, leading to a credible prediction of sea ice variability as climate warms.

The snow/ice albedo is a function of surface characteristics, spectral bands, solar zenith angle, and atmospheric properties. Surface characteristics that influence the snow/ice albedo includes snow depth, ice thickness, snow/ice metamorphosis and impurity, melt pond fraction and depth, and lead fraction. Currently, a diversity of snow/ice albedo parameterizations is used in climate models (see Barry, 1996; Curry *et al*., 2001 for reviews). Most parameterizations are very simple, depending on surface type (open water, bare ice, and snow) and/or surface temperature. A few parameterizations consider

*Correspondence to: Jiping Liu, School of Earth & Atmospheric Sciences Georgia Institute of Technology Atlanta, GA 30332-0340, USA. E-mail: jliu@eas.gatech.edu

Copyright © 2006 Royal Meteorological Society

snow depth, ice thickness, spectral band (visible and near infrared bands), and solar zenith angle. As pointed out by Curry *et al*. (2001), most climate modelers have justified using simple snow/ice albedo parameterizations because of the lack of observations against which to evaluate them. However, this situation is gradually improving, because recent field experiments such as the Surface Heat Budget of the Arctic Ocean (SHEBA, Perovich *et al*., 1999a) provide unprecedented opportunities to evaluate snow/ice albedo parameterizations.

Toward addressing this issue, Curry *et al*. (2001) evaluated different snow/ice albedo parameterizations using a single-column sea ice model. In this paper, we extend Curry's study to a basin-scale dynamic-thermodynamic sea ice model. The general strategy is to extract four different snow/ice albedo parameterizations from a hierarchy of models (Table I, representing the spectrum of parameterizations used in stand-alone sea ice models, numerical weather prediction and regional climate models of the Arctic Basin, and coupled global climate models), and use the high quality *in situ* measurements (surface temperature, snow depth and ice thickness) obtained from SHEBA as input values for the four albedo parameterizations. Then, the parameterized albedos are compared to the SHEBA observed albedo. The importance of systematic biases in the input values in influencing the parameterized albedos is also assessed, which is another important extension from Curry's study. Finally, we examine the impacts of the differences in the albedo parameterizations on sea ice processes using a stand-alone basin-scale dynamic/thermodynamic sea ice model.

2. DATA AND ALBEDO PARAMETERIZATIONS

2.1. Observational data

The SHEBA experiment, which included a year-long (2 October 1997 to 11 October 1998) field program centered on a drifting ice station in the Beaufort Sea, has arguably provided the highest quality suite of surface properties ever made in the Arctic Ocean (Perovich *et al*., 1999a). Measurements of surface temperature, snow depth, ice thickness, and surface albedo obtained from the SHEBA atmospheric surface flux group (ASFG) and Snow and Ice Studies CD-ROM were used in this study (see Persson *et al*., 2002; Perovich *et al*., 1999b for detailed information on the SHEBA data measurements). The time period selected for this evaluation is from 24 May, 1998 to 28 September, 1998 (hereafter referred to as the entire time period), since that it had the highest sampling frequency during rapid surface albedo evolution.

Surface temperature was measured at the SHEBA ASFG site using an Eppley radiometer, which is accurate to within 0.5 °C. Measurements were made every 5 s from May to September, and the daily averaged values were used in this study. The onset of summer melt started on 29 May, as indicated by the surface temperature reaching 0 °C. Thereafter, the surface temperature

Table I. Formulations of four snow/ice albedo parameterizations.

	Dependence	
PW79	Surface type (snow or ice)	Bare ice: $\alpha_i = 0.5(H_s \le 0m)$, snow: $\alpha_s = 0.75$ $(H_s > 0m)$
HIRHAM	Surface temperature	$\alpha = \alpha_{max} - \exp(-(T_m - T_s)/2) \cdot (\alpha_{max} - \alpha_{min})$ where $\alpha_{max} = 0.7, \alpha_{min} = 0.3$
ARCSYM	Surface temperature	Open water: $\alpha_o = 0.1$
	Snow depth	Bare ice: $\alpha_i = 0.55$, snow: $\alpha_s = 0.9$
	Ice thickness	$\alpha_{it} = \alpha_o + \alpha_i \cdot (1 + \tanh((H_i - 0.2)/0.8))/2 - 0.1 \cdot (1 + \tanh((\min(T_s - T_m, T_m) + 1.2)/0.03))/2$
		$\alpha_{st} = \alpha_s - 0.1 \cdot (1 + \tanh((T_s + 1.2)/0.03))/2$
		$\alpha = \alpha_{it}$ $(H_s < 0.01\text{m})$
		$\alpha = \alpha_{it} + H_s/(H_s + 0.1) \cdot (\alpha_{st} - \alpha_{it})$ $(H_s \ge 0.01m)$
		$\alpha = \max(\alpha, \alpha_o + 0.05)$
CCSM3	Spectral bands	Open water: $\alpha_o = 0.06$
	Surface temperature	Bare ice: $\begin{cases} \alpha_{i-vis} = 0.73 \\ \alpha_{i-nir} = 0.33 \end{cases}$, snow: $\begin{cases} \alpha_{s-vis} = 0.96 \\ \alpha_{s-nir} = 0.68 \end{cases}$
	Snow depth	$\alpha_{it-vis} = \alpha_o - \alpha_{i-vis} \cdot \min(a \tan(4 \cdot H_i)/a \tan(2), 1) + 0.075 \cdot \min(T_m - T_s - 1, 0)$
	Ice thickness	$\alpha_{it-nir} = \alpha_o - \alpha_{i-nir} \cdot \min(a \tan(4 \cdot H_i)/a \tan(2), 1) + 0.075 \cdot \min(T_m - T_s - 1, 0)$
		$\alpha_{vis} = \alpha_{it-vis} \cdot (1 - H_s/(H_s + 0.02)) + \alpha_{s-vis} \cdot (H_s/(H_s + 0.02))$
		$\alpha_{nir} = \alpha_{it-nir} \cdot (1 - H_s/(H_s + 0.02)) + \alpha_{s-nir} \cdot (H_s/(H_s + 0.02))$
		$\alpha = 0.53 \cdot \alpha_{vis} + 0.47 \cdot \alpha_{nir}$

where α is albedo, T_s is surface temperature, T_m is melting point (273.15K), H_s is snow depth, H_i is ice thickness, vis(>0.7 μm) and nir(<0.7 μm) are visible and nearinfrared band, respectively.

Copyright © 2006 Royal Meteorological Society

DOI: 10.1002/joc

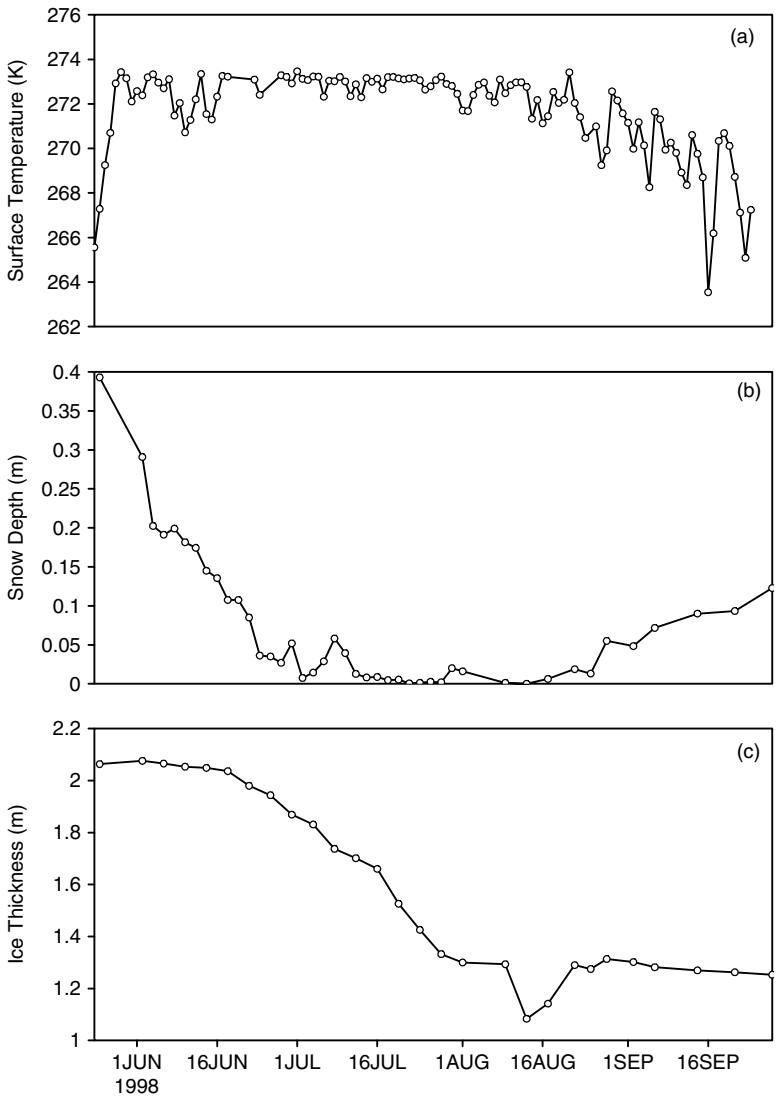

Figure 1. Daily averaged SHEBA observed (a) surface temperature, (b) snow depth, and (c) ice thickness from 24 May, 1998 to 28 September, 1998.

oscillated slightly around the melting point during the summer melt period, and then decreased during the fall freeze-up period (Figure 1(a)).

Snow depth was measured every 1–5 m along a 500-m-long line (Perovich *et al.*, 1999b) either manually using a graduated ski pole or automatically using a magnaprobe, which is accurate to within 0.5 cm. Data is available almost weekly in May and September and every 1–2 days from June to August. The spatially averaged snow depth (all measurements along the 500-m-long line) was computed for each day. As shown in Figure 1(b), there was a steep drop-off in snow depth from late May to mid-June, when most of the snow melted rapidly. Thereafter, only minimal snow depth was present until late summer. Also, there was a great deal of spatial variability in snow depth. For example, snow depth in late May ranged from a few centimeters on the top of a ridge to more than a meter in the lee of a ridge.

Ice thickness was measured at a 50-m-long line (Perovich *et al.*,1999b) using gauges spaced every 2.5 or 5 m. Data is available almost weekly in May and September and every other day from June to August. The spatially averaged ice thickness (all gauges along the 50-m-long line) was computed for each day. Figure 1(c) shows that ice thickness slightly tapered off from late May to mid-June, followed by a steep drop-off during the summer melt period and another tapering in late August and September. Additionally, a brief increase in mid-August might be due to an artifact of fewer gauges (since gauges were not used once the ice broke part dynamically or melted completely).

The wavelength-integrated surface albedo was measured using a Kipp & Zonen albedometer, which is accurate to within 0.01. Albedo measurements were made at least weekly from May to September (but every other day from June to August), and at every 2.5 m along a 200-m-long line (Perovich *et al.*,1999b) that encompassed different snow and ice conditions over multiyear sea ice. The values for each day were used to compute a really averaged albedo (all measurements along

Copyright © 2006 Royal Meteorological Society

DOI: 10.1002/joc

the 200-m-long line). In spring, this line was completely snow covered, and the albedo was high (~0.8–0.9) and spatially uniform. As the melt season progressed, the snow cover diminished, the bare ice developed a melting surface granular layer, the melt ponds grew deeper and wider, and the albedo decreased everywhere along the line. By mid-July, the averaged albedo along the line was ~0.4, and there was significant spatial variability, with values ranging from ~0.1 for deep, dark ponds to ~0.65 for bare, white ice (Figure 2).

2.2. *Descriptions of albedo parameterizations*

Table I lists four snow/ice albedo parameterizations chosen for this study, ranging from simple to complex.

A parameterization of Parkinson and Washington (1979), hereafter referred to as PW79, represents the simplest albedo parameterization, which only includes broadband values of albedo for two different surface types: snow and bare ice. Adding one more layer of complexity, some parameterizations consider an albedo that varies with surface temperature. A model that parameterizes the albedo in this fashion is the Alfred Wegener Institute Regional Climate Model for the Arctic Region (Rinke, personal communication, 2004; Dethloff *et al.*, 1996; hereafter referred to as HIRHAM). In addition to a dependence on the surface temperature, a few parameterizations include variations associated with snow depth and ice thickness. The Arctic Regional Climate System Model (Lynch *et al.*, 1995; hereafter referred to as ARCSYM) is one model using this type of parameterizations. To date, the most sophisticated albedo parameterization used in current-day climate models is found in the National Center for Atmospheric Research Community Climate System Model version 3 (hereafter referred to as CCSM3). In addition to including dry and wet snow, thin, thick and melting ice, and weighted snow and ice albedos using snow depth, this parameterization distinguishes visible and near-infrared albedos (Briegleb *et al.*, 2004).

3. EVALUATION

Figure 2 is a comparison of the observed and parameterized surface albedos during the entire time period. It is noted that the SHEBA observed surface conditions (surface temperature, snow depth, and ice thickness) are used as input values for the four albedo parameterizations to calculate the parameterized surface albedos. The PW79 parameterization greatly overestimates the albedo and cannot capture the observed variations in the albedo. The discrepancy is acute in the summertime, since the PW79 parameterization is tied to the snow depth (Table I), which is still a few centimeters even in the summertime (Figure 1(b)).

The HIRHAM parameterization, which is a function of the surface temperature, greatly underestimates the albedo, and cannot reproduce the observed gradual decrease in the albedo during the summer melt period associated with the changes of surface characteristics. The parameterized albedo mainly oscillates around 0.35, since the surface temperature, the only dependent variable in the HIRHAM parameterization, mainly fluctuates around the melting point during the summer melt period (Figure 1(a)). However, the parameterized albedo reproduces the observed gradual increase in the albedo during the fall freeze-up period.

What is the sensitivity of this parameterization to a systematic bias in the input surface temperature? During the entire time period, the standard deviation of the SHEBA surface temperature is ~1.3 °C, and the magnitude of biases found in the surface temperature of the satellite-based products and reanalyses is ~1–2 °C as compared to the SHEBA surface temperature (Liu *et al.*, 2005). On the basis of that finding, we shift the input SHEBA surface temperature up and down by 1 °C, respectively. For the warm bias case, the parameterized albedo decreases by ~0.2, and the magnitude of the variability is amplified. By contrast, for the cold bias case, the parameterized albedo increases by ~0.15, and the magnitude of the variability is damped. Interestingly,

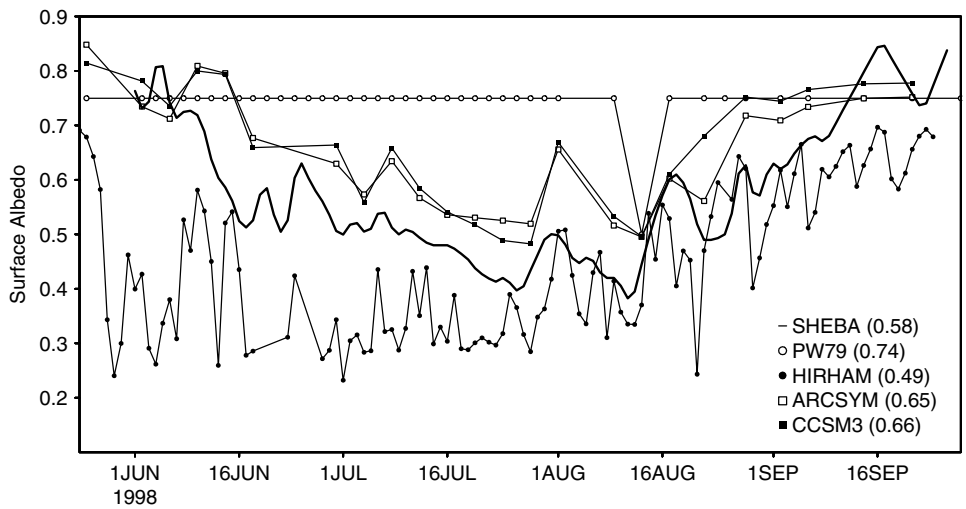

Figure 2. Daily averaged SHEBA observed surface albedo, and parameterized surface albedos for PW79, HIRHAM, ARCSYM, and CCSM3 from 24 May, 1998 to 28 September, 1998 (the mean albedos for the four parameterizations over the entire period is shown in parentheses).

Copyright © 2006 Royal Meteorological Society

DOI: 10.1002/joc

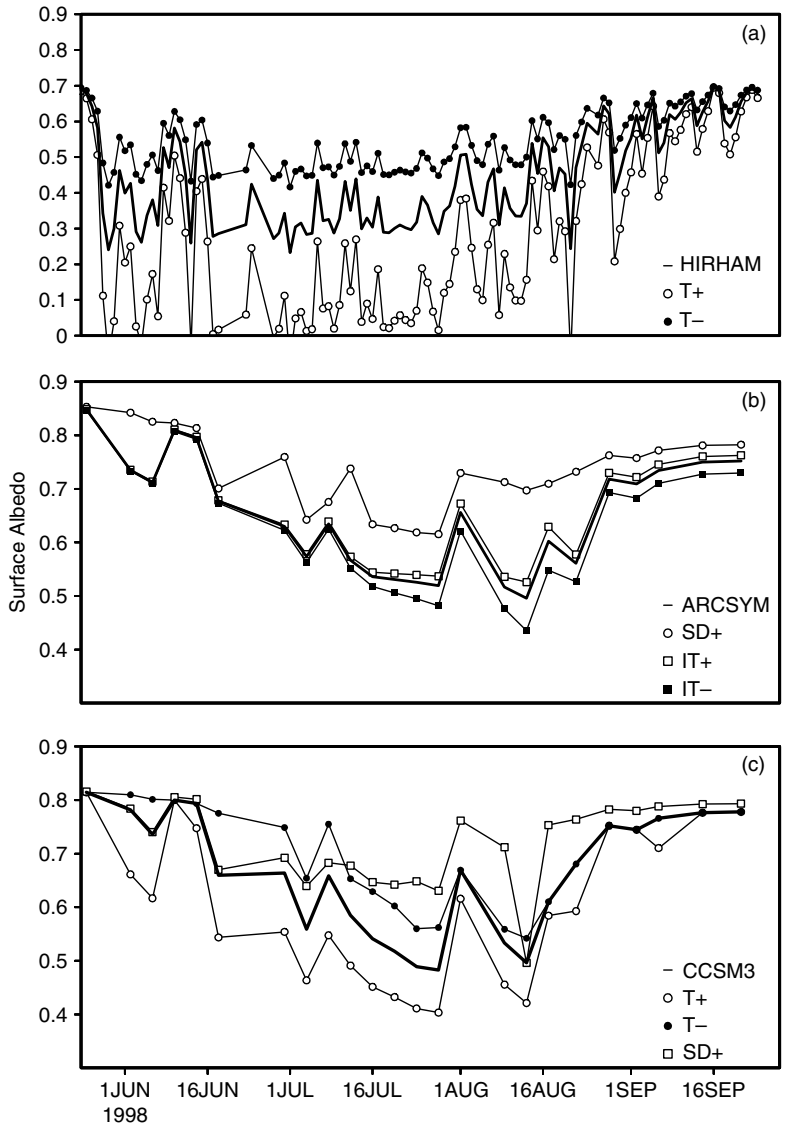

Figure 3. Parameterized surface albedos for (a) HIRHAM, (b) ARCSYM, and (c) CCSM3 given the systematic biases in the input parameters, T + (T−1): surface temperature shift up (down), SD+: snow depth shift up, IT + (IT−): ice thickness shift up (down).

the difference between the parameterized albedo of the cold bias case (Figure 3(a), closed circle) and the SHEBA observed albedo is approximately half that seen in the warm bias case (Figure 3(a), open circle). The parameterized albedo of the cold bias case even has smaller differences than the case using the actual SHEBA surface temperature (Figure 3(a), thick sold line). This suggests that introducing a cold bias to the input surface temperature for the HIRHAM parameterization actually produces better albedo simulations.

The ARCSYM parameterization, which depends on the surface temperature, snow depth and ice thickness, captures the quality of the observed seasonal fluctuations in the albedo, particularly during the summer melt period as compared to the PW79 and HIRHAM parameterizations (Figure 2). However, the parameterized albedo never falls below 0.5, whereas the SHEBA observed albedo was well below 0.5 from mid-July to mid-August. This discrepancy is due to the SHEBA measurement (albedo line) probably overestimates the melt pond fraction (Perovich *et al.*, 2002). Additionally, it cannot capture the observed quick drop-off in the albedo in early June associated with the formation of melt ponds. For this parameterization, the 1 °C bias in the input SHEBA surface temperature does not influence the parameterized albedo greatly (not shown). We further examined the sensitivity of the ARCSYM parameterization to the systematic biases in snow depth and ice thickness. During the entire time period, the standard deviation of the SHEBA snow depth and ice thickness is ~0.07 m and ~0.35 m, respectively. On the basis of that finding, we shift up the input SHEBA snow depth slightly by 0.05 m. The parameterized albedo increases by ~0.12, and cannot reproduce the observed low albedo during the summer melt period (Figure 3(b)). By shifting the input SHEBA ice thickness up and down by 0.35 m, respectively, the parameterized albedo also increase and decrease slightly, respectively. The parameterized albedo is more sensitive to the negative bias in

Copyright © 2006 Royal Meteorological Society

DOI: 10.1002/joc

ice thickness in mid-July and August, but there is little sensitivity to the shifts in May and June (Figure 3(b)).

Despite being the most complex parameterization, the CCSM3 parameterization, which includes spectral dependence (see Table I for details), shows similar albedo variations to the ARCSYM parameterization. However, the CCSM3 parameterization has quite different sensitivity to the aforementioned biases in the input surface temperature and ice thickness relative to the ARCSYM parameterization. Specifically, the CCSM3 parameterization shows similar sensitivity to the 1 °C bias in the input SHEBA surface temperature as the HIRHAM parameterization, albeit of smaller magnitude (Figure 3(c)). The 0.35 m bias in the input SHEBA ice thickness has no influence on the parameterized albedo (not shown).

The fact that both the ARCSYM and CCSM3 parameterizations overestimate the albedo during the melt season raises the possibility that important processes are being underestimated. Since melt ponds play a substantial role during that time period, they need to be given further consideration and be explicitly described in the snow/ice albedo parameterizations. This will be addressed in future research.

To further examine which input parameter – surface temperature, snow depth or ice thickness – is more important in determining the surface albedo, we calculated correlations between the albedo and each parameter using the SHEBA measurements. The correlation between the albedo and ice thickness is 0.18, which is much smaller than the correlations between the albedo and (1) the surface temperature and (2) snow depth, which are −0.64 and 0.76, respectively. Partial correlation was then used to further determine relative influences of the surface temperature and snow depth on the albedo. The partial correlation of the albedo and surface temperature, with the effects of snow depth removed is reduced to −0.29. By contrast, the partial correlation of the albedo and snow depth, with the effects of the surface temperature removed still maintains a high value (0.61). This indicates that snow depth plays a relatively more important role than the surface temperature and ice thickness in determining the albedo, and should be included in the albedo parameterizations.

4. IMPACTS OF ALBEDO PARAMETERIZATIONS ON SEA ICE SIMULATIONS

To further explore impacts of the differences in the snow/ice albedo parameterizations on sea ice processes, we examined the sensitivity of a stand-alone basin-scale dynamic/thermodynamic sea ice model to the PW79, HIRHAM, ARCSYM, and CCSM3 albedo parameterizations. Specifically, we examined impacts of variations in the parameterized albedos on the simulations of baseline sea ice characteristics. Also, responses of sea ice to an external perturbation were compared.

For the basin-scale sea ice model, we used the Los Alamos sea ice model (CICE, http://climate.lanl.gov/Models/CICE). It features elastic-viscous-plastic ice dynamics (Hunke and Dukowicz, 1997), horizontal advection via a new incremental remapping scheme based on Dukowicz and Baumgardner (2000), an energy conserving thermodynamics model (Bitz and Lipscomb, 1999) with one layer of snow and four layers of ice in each of the five ice thickness categories, a penetration of solar radiation in the snow/ice and ocean (http://climate.lanl.gov/Models/CICE), an energy-based ridging scheme of Thorndike *et al.* (1975), and an ice strength parameterization given by Rothrock (1975). Prognostic variables for each thickness category include ice area fraction, ice volume, ice energy in each vertical layer, snow energy, and surface temperature. A nonlinear, vertical salinity profile remains constant. The temperature dependence of longwave radiation, and sensible and latent heat fluxes is included in the nonlinear flux balance that (iteratively) determines the snow or ice surface temperature. An ocean mixed-layer formulation is included in CICE, which determines the mixed-layer variables (i.e. temperature and salinity).

Two different CICE simulations are conducted for the aforementioned albedo parameterizations: (1) a baseline simulation, representing the unperturbed climate condition; and (2) a simulation in which the climate is subject to a positive perturbation to the surface downward longwave radiative flux on the magnitude of 4 W/m^2, which is comparable to the direct doubled CO_2 forcing of 4 W/m^2 (Ramanathan *et al.*, 1989). Each simulation was run for 15 years, following a 15-year spinup period. The simulations were forced by the specified atmospheric forcings from the NCEP (National Center for Environmental Prediction) reanalysis II in 1997 (annually repeating forcing, including surface air temperature, humidity and density, surface downward shortwave and longwave radiation, surface winds and precipitation). As suggested by some studies (Curry *et al.*, 2001; Liu *et al.*, 2005), there are uncertainties in the NCEP atmospheric forcing. However, by comparing model simulations with each other (as opposed to with observations), we can minimize uncertainties caused by the atmospheric forcing, and highlight impacts due to the differences in the snow/ice albedo parameterizations. CICE is run on the (Parallel Ocean Program) POP displaced pole grid, at a resolution of $\sim$1.6°(latitude) × 3.6° (longitude). Results are shown for the average over the last 3 years of the simulations.

Figures 4 and 5(a) show the averaged simulated surface albedos from June to September. Because the aforementioned albedo parameterizations interact with the simulated surface features in different ways, the simulated surface albedos differ substantially. The simulation using the simplest parameterization (PW79) produces an excessively high and spatially uniform albedo ($\sim$0.75, because of the presence of small amounts of snow in the summertime in the NCEP reanalysis), leading to a much colder mixed layer (< -1.8 °C) and more extensive ice concentrations (>80%) in the entire Arctic Ocean than those produced by other parameterizations (HIRHAM, ARCSYM, and CCSM3).

Copyright © 2006 Royal Meteorological Society

DOI: 10.1002/joc

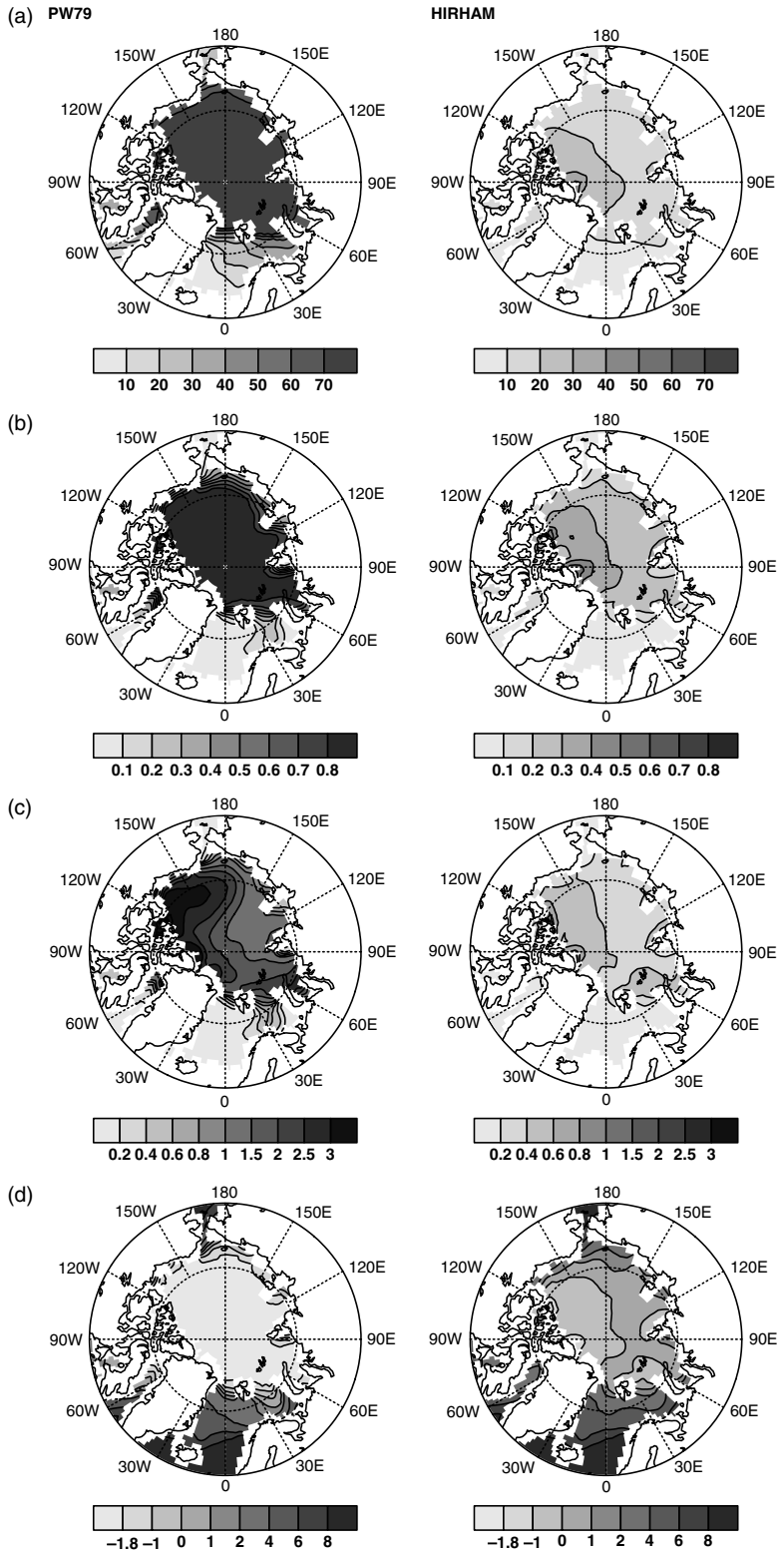

Figure 4. Averaged simulated surface albedo (a), ice cover (b), ice thickness (c), and ocean mixed-layer temperature (d) from June to September for PW79 (left column) and HIRHAM (right column).

The albedos in the HRIHAM, ARCSYM, and CCSM3 simulations all show similar spatial variability. The albedos increase from the Chukchi Sea and East Siberian Sea to the Canadian Archipelago, and from the Greenland-Iceland-Norwegian Sea to the Barents Sea. However, the albedo in the HIRHAM simulation is much smaller than that in the ARCSYM and CCSM3 simulations, as noted in Section 3. The much smaller albedo in the HIRHAM simulation allows more incoming shortwave radiation to be transmitted to the ocean, which results in a warmer ocean mixed layer, as shown in Figure 4(d). This increases the ice melting (not shown), leading to less ice

Copyright © 2006 Royal Meteorological Society

DOI: 10.1002/joc

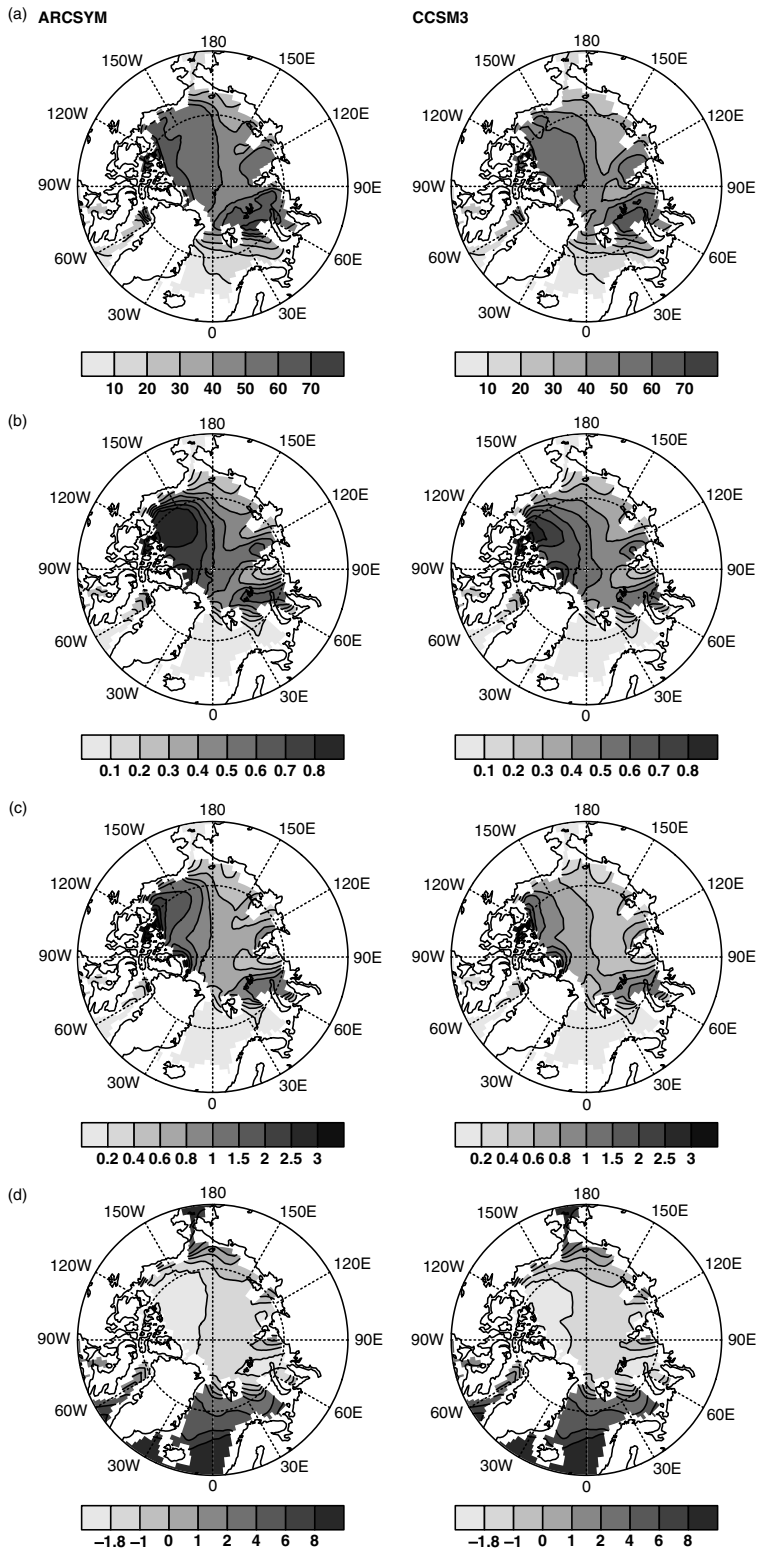

Figure 5. Averaged simulated surface albedo (a), ice cover (b), ice thickness (c) and ocean mixed-layer temperature (d) from June to September for ARCSYM (left column) and CCSM3 (right column).

concentration and thinner ice thickness in the HIRHAM simulation than in the ARCSYM and CCSM3 simulations ((b) and (c) of Figure 5). Moreover, the HIRHAM simulation produces weaker ice thickness gradient from the Canadian Archipelago to the Eurasian basin as compared to the PW79, ARCSYM, and CCSM3 simulations (Bourke and Garrett, 1987), which is partly because the ice is far too thin toward North America. Too thin ice toward North America in the HIRHAM simulation relative to other simulations is because the albedo toward North America in the HIRHAM simulation is ~0.4 lower than that of the ARCSYM and CCSM3 simulations,

Copyright © 2006 Royal Meteorological Society

DOI: 10.1002/joc

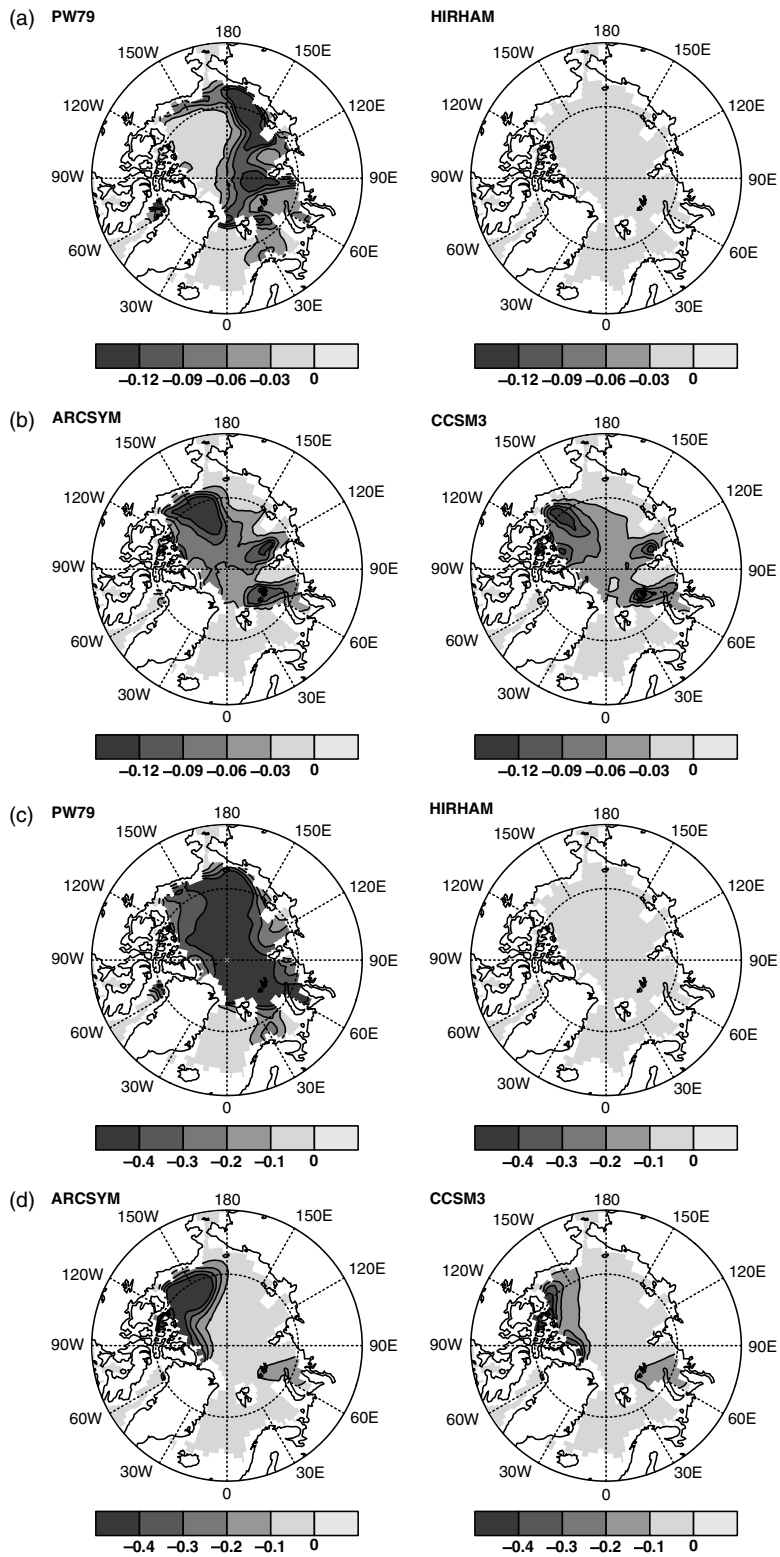

Figure 6. Averaged response of ice cover ((a) and (b)) and thickness ((c) and (d)) from June to September to an external perturbation for PW79, HIRHAM, ARCSYM, and CCSM3 (as compared to the baseline simulations in Figures 4 and 5).

which is two times larger than the albedo difference toward Eurasia. As a consequence of much lower albedo and more incoming shortwave radiation to be transmitted to the ocean, the ocean mixed-layer temperature toward North America in the HIRHAM simulation is ~0.6 °C above the freezing point (~ −1.8 °C), whereas it is near freezing for the ARCSYM and CCSM3 simulations. These greatly enhance both surface and basal ice melting.

Figure 6 shows the responses of sea ice cover ((a) and (b)) and thickness ((c) and (d)) to a 4 W/m^2 increase in the surface downward longwave radiative flux as

Copyright © 2006 Royal Meteorological Society

DOI: 10.1002/joc

compared to the baseline simulations (Figures 4 and 5). The ice cover and thickness in the HIRHAM simulation show small and spatially uniform responses to the perturbation. Specifically, the ice cover and thickness in the entire Arctic Ocean decrease less than 2% and 0.05 m, respectively. By contrast, the ice cover and thickness in the PW79, ARCSYM, and CCSM3 simulations show regionally varying responses to the perturbation. The simulation using the simplest parameterization (PW79) has a very different spatial pattern than the other two (ARCSYM and CCSM3), with (1) the ice cover in the eastern Arctic showing a much larger response (>10%) than that in the western Arctic, and (2) large and quite spatially uniform responses in ice thickness (>0.4 m) in almost the entire Arctic Ocean. Interestingly, the CCSM3 simulation, whose parameterization includes the dependence on spectral band, shows regional responses very similar to the ARCSYM simulation. For both the ARCSYM and CCSM3 simulations, the ice cover in the Beaufort Sea, Laptev Sea, and Barents Sea is more sensitive (decreases by ~8%) than other regions, while the ice thickness extending from the Beaufort Sea to the northern Greenland Sea is more sensitive (decreases by ~0.35 m) than other regions.

5. CONCLUSIONS

This study evaluated four different snow/ice albedo parameterizations (see Table I), representing the types of parameterizations used in stand-alone sea ice models, numerical weather prediction and regional climate models of the Arctic Basin, and coupled global climate models), and examined their impacts on sea ice simulations.

By comparing the parameterized surface albedo (inputting the SHEBA measured surface conditions into the four albedo parameterizations) to the SHEBA observed surface albedo, we found that these parameterizations give very different representations of surface albedo from late spring to early fall. In general, more complex albedo parameterizations depending on snow depth and spectral band can yield more realistic variations in the albedo than those depending solely on surface types or surface temperature, particularly during the summer melt period. Both the ARCSYM and CCSM3 parameterizations are very sensitive to the systematic bias in snow depth, but show little sensitivity to the surface temperature and ice thickness, respectively.

The importance of the complexity of the albedo parameterizations in the determination of the baseline sea ice simulations was also examined. It is found that the albedo treatment only depending on the surface types (the surface temperature), like PW79 (HIRHAM), produces very high (low) surface albedo, leading to extensive ice concentrations over the entire Arctic Ocean (unrealistic basin-scale ice thickness distribution).

The perturbation simulations using the CICE sea ice model further emphasized the importance of the complexity of the albedo parameterizations. It is found that more complex albedo treatments, like ARCSYM and CCSM3, show that the ice thickness extending from the Beaufort Sea to the northern Greenland Sea is more sensitive than other regions to the external perturbation (Figure 6). Submarine measurements exhibit a similar behavior, as first-year ice has become more prevalent during the period 1993–1997 as compared to the period 1958–1970, at the expense of a decreasing probability of thick ridged ice (Yu *et al.*, 2004). The satellite-based observations also show that the perennial ice cover in the Arctic has declined at a much faster rate than the annual mean ice cover (Comiso, 2002). Thus, the simulated ice cover and thickness using more complex albedo treatments (ARCSYM and CCSM3) give more realistic regionally varying sensitivity to the perturbation, whereas the simpler albedo treatments show either spatially uniform (HIRHAM) or unrealistic regional (PW79) sensitivity. Therefore, it is important to include an albedo treatment of sufficient complexity in climate models to reproduce realistic ice albedo feedback, and radiative exchanges between the atmosphere and ocean/sea ice, leading most likely to more realistic ice responses as climate warms.

While it is well accepted that the Arctic may experience amplified warming under CO_2 doubling conditions, current-day climate models provide a broad spectrum of warming estimates, ranging from 1.5 to 4.5 times the global mean warming (Holland and Bitz, 2003). Besides sea ice albedo feedback, Holland and Bitz (2003) identified a number of physical processes that have strong impacts on sea ice simulations, and contribute to the polar amplification and its variations in climate models (i.e. cloud coverage and ocean heat transport). Here, quantifying and understanding the snow/ice albedo parameterizations (sea ice albedo feedback) and their impacts on sea ice simulations are the first step toward reducing the uncertainty in projections of high-latitude climate change. Our future research will explore how much of this range can be attributed to differences in the snow/ice albedo parameterizations used by current-day climate models. Toward that end, we will employ different snow/ice albedo parameterizations (simple to complex) in the same-coupled global climate model, and examine the range of warming responses in the Arctic.

ACKNOWLEDGEMENTS

This research was supported by NASA, The 'Hundred Talent Program' of the Chinese Academy of Sciences, and the National Natural Science Foundation of China under grant 40233032. We thank A. Rinke (HIRHAM) and J. Cassano (ARCSYM) for providing the snow/ice albedo parameterizations.

REFERENCES

Barry RG. 1996. The parameterization of surface albedo for sea ice and its snow cover. *Progress in Physical Geography* **20**: 63–79.

Bitz CM, Lipscomb WH. 1999. An energy-conserving thermodynamic sea ice model for climate study. *Journal of Geophysical Research* **104**: 15–669–15–677.

Copyright © 2006 Royal Meteorological Society

Bourke RH, Garrett RP. 1987. Sea-ice thickness distribution in the Arctic Ocean. *Cold Regions Science and Technology* **13**: 259–280.

Briegleb BP, Bitz CM, Hunke EC, Lipscomb WH, Schramm JL. 2004. *Scientific Description of the Sea ice Component in the Community Climate System Model*, version three, http://www.ccsm.ucar.edu/models/ccsm3.0/csim.

Comiso JC. 2002. A rapidly declining perennial sea ice cover in the Arctic. *Geophysical Research Letters* **29**: 1956 DOI:10.1029/2002GL015650.

Curry JA, Schramm JL, Ebert EE. 1995. On the sea ice albedo climate feedback mechanism. *Journal of Climate* **8**: 240–247.

Curry JA, Schramm JL, Perovich DK, Pinto JO. 2001. Applications of SHEBA/FIRE data to evaluation of snow/ice albedo parameterizations. *Journal of Geophysical Research* **106**: 15345–15355.

Dethloff K, Rinke A, Lehmann R, Christensen JH, Botzet M, Machenhauer B. 1996. A regional climate model of the Arctic atmosphere. *Journal of Geophysical Research* **101**: 23401–23422.

Dukowicz JK, Baumgardner JR. 2000. Incremental remapping as a transport/advection algorithm. *Journal of Computational Physics* **160**: 318–335.

Holland MM, Bitz CM. 2003. Polar amplification of climate change in coupled models. *Climate Dynamics* **21**: 221–232.

Houghton JT, Ding Y, Griggs DJ, Noguer M, Van der Linden PJ, Dai X. 2001. *Climate Change 2001: The Scientific Basis*. Cambridge, University Press: Cambridge.

Hunke EC, Dukowicz JK. 1997. An elastic-viscous-plastic model for sea ice dynamics. *Journal of Physical Oceanography* **27**: 1849–1867.

Ingram WJ, Wilson CA, Mitchell JFB. 1989. Modeling climate change: an assessment of sea ice and surface albedo feedbacks. *Journal of Geophysical Research* **94**: 8609–8622.

Liu J, Curry JA, Rossow WB, Key JR, Wang X. 2005. Comparison of surface radiative flux data sets over the Arctic Ocean. *Journal of Geophysical Research* **110**: C02015, DOI:10.1029/2004JC002381.

Lynch AH, Chapman WL, Walsh JE, Weller G. 1995. Development of a regional climate model of the western Arctic. *Journal of Climate* **8**: 1555–1570.

Parkinson CL, Washington WM. 1979. A large scale numerical model of sea ice. *Journal of Geophysical Research* **84**: 311–337.

Perovich DK, Grenfell TC, Light B, Hobb PV. 2002. Seasonal evolution of the albedo of multiyear Arctic sea ice. *Journal of Geophysical Research* **107**: 8044 DOI:10.1029/2000JC000438.

Perovich DK, Coauthors. 1999a. Year on ice gives climate insights. *EOS, Transactions of the American Geophysical Union* **80**: 485–486.

Perovich DK, Grenfell TC, Light B, Richter-Menge JA, Sturm M, Tucker WB III, Eicken H, Maykut GA, Elder B. 1999b. *SHEBA: Snow and Ice Studies CD-ROM*: Hanover, NH.

Persson POG, Fairall CW, Andreas E, Guest P, Perovich DK. 2002. Measurements near the atmospheric surface flux group tower at SHEBA: near-surface conditions and surface energy budget. *Journal of Geophysical Research* **107**: 8045 DOI:10.1029/2000JC000705.

Ramanathan V, Cess RD, Harrison EF, Minnis P, Barkstrom BR, Ahmad E, Hartman D. 1989. Cloud-radiative forcing and climate: results from the earth radiation budget experiment. *Science* **243**: 57–63.

Rothrock DA. 1975. The energetics of the plastic deformation of pack ice by ridging. *Journal of Geophysical Research* **80**: 4514–4519.

Thorndike AS, Rothrock DA, Maykut GA, Colony R. 1975. The thickness distribution of sea ice. *Journal of Geophysical Research* **80**: 4501–4513.

Washington WW, Meehl GA. 1986. General circulation model CO2 sensitivity experiments: snow-sea ice albedo parameterizations and globally averaged surface air temperature. *Climatic Change* **8**: 231–241.

Yu Y, Maykut GA, Rothrock DA. 2004. Changes in the thickness distribution of Arctic sea ice between 1958–1970 and 1993–1997. *Journal of Geophysical Research* **109**: DOI:10.1029/2003JC001982.

Copyright © 2006 Royal Meteorological Society